Thermochimica Acta 493 (2009) 90–95

Contents lists available at ScienceDirect

Thermochimica Acta

journal homepage: www.elsevier.com/locate/tca

Thermal degradation kinetics of *g*-HA/PLA composite

Jia Li[a,b], Wei Zheng[a], Li Li[a], Yufeng Zheng[a,*], X. Lou[a,c]

[a] *Center for Biomedical Materials and Engineering, Harbin Engineering University, Harbin 150001, China*
[b] *School of Chemistry and Environmental Engineering, Harbin University of Science and Technology, Harbin 150040, China*
[c] *Department of Chemical Engineering, Curtin University of Technology, Kent Street, Bentley WA9102, Australia*

ARTICLE INFO

Article history:
Received 28 January 2009
Received in revised form 13 April 2009
Accepted 15 April 2009
Available online 23 April 2009

Keywords:
Polylactide
Hydroxyapatite
Invariant kinetic parameters method
Thermal degradation

ABSTRACT

Thermal degradation behaviors of a composite constituted by poly(*l*-lactide) (PLA) and hydroxyapatite nanoparticle that was surface-grafted with *l*-lactic acid oligomer (*g*-HA) in a nitrogen atmosphere were studied using thermogravimetric analysis (TGA) and compared with PLA. The kinetic models and parameters of the thermal degradation of PLA and the *g*-HA/PLA composite were evaluated by the invariant kinetic parameters (IKP) method and Flynn–Wall–Ozawa (FWO) method based on a set of TGA data obtained at different heating rates. It was shown that the conversion functions calculated by means of the IKP method depend on a set of kinetic models. The *g*-HA particle slowed down the thermal degradation of PLA polymer matrix.

1. Introduction

In recent years, hydroxyapatite (HA) nanoparticles have been widely used as reinforcing fillers in biomedical materials [1–6]. Among them, hydroxyapatite/poly(*l*-lactide) (HA/PLA) composites have been studied in various forms due to the good osteoconductivity of HA and biodegradability of PLA [7–9]. For an ordinary HA/PLA composite system, the interaction between the HA filler and the PLA matrix is a critical factor in determining the mechanical properties and extending the applications of the composite. A simple physical adsorption between the two phases might result in an early failure at the interface and thus deteriorate the mechanical properties. Various substances, including different coupling agents [10,11] and organic isocyanates [12], have been investigated in the past to increase the interfacial strength between the inorganic particle and the polymeric matrix. This often induces some foreign substances into the materials which might not be entirely desirable for the applications.

In our recent work, a method to improve the interfacial adhesion between the HA particle and the PLA matrix has been developed [13]. The surface of HA particles was first grafted with *l*-lactic acid oligomer through chemical bonding and then further blended with the PLA matrix. The results demonstrated that *g*-HA particles were well dispersed in PLA matrix than unmodified HA particles. And *g*-HA/PLA composites showed good mechanical properties than that of unmodified HA/PLA. In view of the productions and applications of these materials, further studies should be developed to determine the thermal stability as well as to allow a better understanding on the mechanism and kinetics involved in the thermal degradation of the composite. However, there is no information in the open literature about the thermal degradation mechanism of the *g*-HA composite. The aim of the present work is to study the thermal degradation of the *g*-HA composite and to evaluate its kinetic parameters of thermal degradation during heating in an inert atmosphere.

Thermogravimetric analysis is one of the most commonly used methods to study the thermal degradation kinetics of materials. The complexity of the thermal degradation of PLA and its composites has been reported by some workers [14–19]. According to McNeill and Leiper [14], the main reaction route of PLA degradation is a non-radical, backbiting ester interchange reaction. They reported that the main products were cyclic oligomers, including lactide. Other lower boiling point products, such as acetaldehyde, ketene, carbon dioxide, and carbon monoxide were also produced. They employed a 1st-order reaction kinetic equation to calculate the apparent activation energy, *E*, as 119 kJ/mol. Kopinke et al. [15] have suggested that degradation of PLA at temperatures above 200 °C includes intra-molecular transesterification leading to cyclic oligomers, cis-elimination leading to acrylic acid, and fragmentation leading to acetaldehyde and CO_2. And they found that intra-molecular transesterification was a dominant degradation pathway. Aoyagi et al. [16] found that the *E* values of PLA changed in the range 80–160 kJ/mol with the weight loss. And they concluded that the pyrolysis of PLA involved more than two mechanisms.

* Corresponding author at: Center for Biomedical Materials and Engineering, Harbin Engineering University (Building 11#), No. 145, Na-Tong-Da Street, Nan-Gang District, Harbin 150001, China. Tel.: +86 451 82518644; fax: +86 451 82518644.
E-mail address: yfzheng@hrbeu.edu.cn (Y. Zheng).

0040-6031/$ – see front matter © 2009 Elsevier B.V. All rights reserved.
doi:10.1016/j.tca.2009.04.009

Babanalbandi et al. [17] studied the thermal degradation behavior of PLA using isothermal methods. The results showed that at first the E value decreased from 103 to 72 kJ/mol with an increase of weight loss and then increased up to 97 kJ/mol. It concluded that the PLA degradation process follows more complex kinetics. Wu et al. [18] studied multi-walled carbon nanotubes (MWCNTs)/PLA nanocomposites and concluded that the presence of MWCNTs had little influence to the thermal stability at the initial stage of degradation, but improved slightly the thermal stability at a higher decomposition level. Another study by Wu et al. [19] indicated that the thermal stability of polylactide/clay nanocomposites (PLACNs) decreases with the addition of clay, in contrast to that of pure PLA.

In this paper, thermal degradation of g-HA/PLA composite was studied under nitrogen at different heating rates. The kinetic parameters (activation energy E and pre-exponential factor A) and the mechanism for their thermal degradation were evaluated with the data processing performed by using well-known methods, i.e. Flynn–Wall–Ozawa method (FWO method) [20,21] and the invariant kinetic parameters method (IKP method) [22,23]. The influence of g-HA particles on the thermal stability, kinetic parameters and the degradation rate of the PLA matrix was also discussed.

2. Theoretical consideration

A typical model for a kinetic process of an isothermal degradation can be expressed as:

$$\frac{d\alpha}{dt} = kf(\alpha) \tag{1}$$

where α is the conversion degree ($\alpha = (W_0 - W_t)/(W_0 - W_f)$, W_t, W_0, and W_f are time t, initial and final weights of the sample, respectively), $d\alpha/dt$ is the conversion rate, k is the degradation rate constant and $f(\alpha)$ is the differential expression of a kinetic model function, which depends on the particular degradation mechanism.

According to Arrhenius equation:

$$k = A\exp\left(-\frac{E}{RT}\right) \tag{2}$$

where A is the pre-exponential factor (s^{-1}), assumed to be independent of temperature, E is the activation energy (kJ mol^{-1}), T is the absolute temperature (K), and R is the gas constant (8.314 J mol^{-1} K^{-1}).

Substituting "k" from Eq. (2) into Eq. (1) obtains:

$$\frac{d\alpha}{dt} = A\exp\left(-\frac{E}{RT}\right)f(\alpha) \tag{3}$$

For non-isothermal measurements at constant heating rate $\beta = dT/dt$, Eq. (3) transforms to

$$\frac{d\alpha}{dT} = \frac{A}{\beta}\exp\left(-\frac{E}{RT}\right)f(\alpha) \tag{4}$$

Eqs. (3) and (4) are the fundamental expressions of analytical methods to calculate kinetic parameters on the basis of TG data.

2.1. Flynn–Wall–Ozawa method (FWO method)

FWO method [20,21] is an integral method that can determine the activation energy without any knowledge of the reaction mechanisms. It used the following approximate equation at a constant weight loss in a thermal degradation process:

$$\log\beta = \log\frac{AE}{g(\alpha)R} - 2.315 - \frac{0.4567E}{RT} \tag{5}$$

where $g(\alpha)$ is the integral mechanism function, $g(\alpha) = \int_0^\alpha d\alpha/f(\alpha)$.

The value of E can be computed by FWO method for any particular degree of conversion. Therefore, according to Eq. (5), plotting $\log(\beta)$ against $1/T$ should give straight lines, the slope of which is directly proportional to the activation energy.

2.2. Coats-Redfern method (CR method)

Coats-Redfern method [24] is also an integral method, and it involves the thermal degradation mechanism. Using an asymptotic approximation ($2RT/E \ll 1$), Coats-Redfern technique uses the following equation for studying the thermal degradation kinetics:

$$\ln\frac{g(\alpha)}{T^2} = \ln\left(\frac{AR}{\beta E}\right) - \frac{E}{RT} \tag{6}$$

E and A can be determined from the slope and the intercept of the straight line $\ln[g(\alpha)/T^2]$ versus $1/T$, respectively.

2.3. The invariant kinetic parameters method (IKP method)

The application of the IKP method [22,23] is based on the study of the compensation effect. For each function $f_j(\alpha)$, $\log(A_j)$ versus E_j is plotted and if a compensation effect is observed, a linear relation is observed for each heating rate β_v:

$$\log A_{jv} = B_v + I_v E_{jv} \tag{7}$$

where A_{jv} and E_{jv} are the apparent pre-exponential factor and activation energy calculated with a function $f_j(\alpha)$ at β_v, respectively.

The values of compensation parameters (B_v and I_v) are then calculated from the slopes and intercepts of the straight lines observed. The significance of B_v and I_v has been discussed by Lesnikovich [25] and it has been demonstrated that:

$$B_v = \log(k_v)$$

$$I_v = (2.3RT_v)^{-1}$$

where k_v is the rate constant of the system at the temperature T_v.

The curves B_v are then plotted against I_v:

$$B_v = \log(A_{inv}) - I_v E_{inv} \tag{8}$$

Thus, the values of the invariant activation energy (E_{inv}) and pre-exponential factor (A_{inv}) can be calculated from the slope and intercept of the curves.

The degradation is often modeled by computing the probabilities associated with 18 degradation functions (Table 1).

Using kinetic parameters E_{inv} and $\log A_{inv}$, a kinetic equation appropriate to the most probable mechanism of a process can be found [26].

The kinetic functions $f_j(\alpha)$ may then be discriminated using the $\log A_{inv}$ and E_{inv} values obtained. Knowing n of the ith experimental values of $(d\alpha/dT)_{iv}$, the residual sum of squares for each $f_j(\alpha)$ and for each heating rate β_v may be computed:

$$(n-1)S_{jv}^2 = \sum_{i=1}^{i=n}\left|\left(\frac{d\alpha}{dT}\right)_{iv} - \frac{A_{inv}}{\beta_v}\exp\left(-\frac{E_{inv}}{RT_{iv}}\right)f_j(\alpha_{iv})\right|^2 \tag{9}$$

The most probable function is then chosen by the average minimum value of $\overline{S_j}$:

$$\overline{S_j} = \frac{1}{p}\sum_{v=1}^{v=p} S_{jv} \tag{10}$$

with p is the number of heating rates used.

The probability associated with each $f_j(\alpha)$ can be calculated by defining the ratio:

$$F_j = \frac{\overline{S_j}^2}{\overline{S}_{\min}^2} \tag{11}$$

Table 1
Degradation functions used in the IKP method.

Kinetic models	$f_j(\alpha)$	$g_j(\alpha)$	
Nucleation and nucleus growing	$\frac{1}{n}(1-\alpha)(-\ln(1-\alpha))^{1-n}$	$(-\ln(1-\alpha))^n$	S1, $n=1/4$ S2, $n=1/3$ S3, $n=1/2$ S4, $n=2/3$ S5, $n=1$
Phase boundary reaction	$(1-\alpha)^n$	$1-(1-\alpha)$ $2[1-(1-\alpha)^{1/2}]$ $3[1-(1-\alpha)^{1/3}]$	S6, plane symmetry S7, cylindrical symmetry S8, spherical symmetry
Diffusion	$\frac{1}{2}\alpha^{-1}$ $[-\ln(1-\alpha)]^{-1}$ $\frac{3}{2}[(1-\alpha)^{-1/3}-1]^{-1}$ $\frac{3}{2}(1-\alpha)^{1/3}[(1-\alpha)^{-1/3}-1]^{-1}$	α^2 $\alpha+(1-\alpha)\ln(1-\alpha)$ $1-\frac{2}{3}\alpha-(1-\alpha)^{2/3}$ $[1-(1-\alpha)^{1/3}]^2$	S9, plane symmetry S10, cylindrical symmetry S11, spherical symmetry S18, Jander's type
Potential law	$\frac{1}{n}\alpha^{1-n}$	$\alpha^n (0<n<2)$	S12, $n=1/4$ S13, $n=1/3$ S14, $n=1/2$ S17, $n=3/2$
Reaction order	$\frac{1}{n}(1-\alpha)^{1-n}$	$1-(1-\alpha)^{1/2}$ $1-(1-\alpha)^{1/3}$	S15, $n=1/2$ S16, $n=1/3$

where $\overline{S}_j^2 = (1/p)\left(\sum_{\nu=1}^{\nu=p}\tilde{S}_{j\nu}^2\right)$ and $\tilde{S}_{\min}^2$ is the average minimum of the residual dispersion.

This ratio obeys the *F*-distribution (Eq. (12)):

$$q(F_j) = \frac{\Gamma(\nu)}{\Gamma^2(\nu/2)} \times \frac{F_j^{(\nu/2)-1}}{(1+F_j)^{\nu}} \tag{12}$$

where ν is the number of degrees of freedom equal for every dispersion and Γ is the Gamma function.

The probabilities of the *j*th function are computed on the assumption that the experimental data with *L* kinetic functions are described by a complete and independent events' systems (Eq. (13)).

$$\sum_{j=1}^{j=L} P_j = 1 \tag{13}$$

Therefore we obtain Eq. (14):

$$P_j = \frac{Z_j}{\sum_{j=1}^{j=L} Z_j} \tag{14}$$

with $Z_j = 1 - \frac{\Gamma(\nu)}{\Gamma^2(\nu/2)} \int_0^{F_j} x^{(\nu/2)-1}(1+x)^{-\nu}\,dx$.

3. Experimental

l-Lactide (LA) was synthesized from *l*-lactic acid (Purac, The Netherlands) according to a reported method [27]. PLA was prepared from LA using stannous octanoate ($Sn(oct)_2$) as catalyst. The product was dissolved in chloroform, precipitated in excess methanol and then dried under vacuum. The molecular weight (M_n) and M_w/M_n of PLA indicated by GPC were 101,271 and 1.82, respectively. The composite of *g*-HA and PLA was prepared as described in our previous work [13]. In brief, a dehydration reaction was carried out between the hydroxyl groups of nano-HA particles and the carboxyl groups of the *l*-lactic acid, producing HA nanoparticles that were modified with *l*-lactic acid. The modified HA particles were then mixed with *l*-lactide and kept at 130 °C for 24 h in a glass ampoule using stannous octoate as a catalyst, to produce *l*-lactic acid oligomer grafted nano-HA, *g*-HA. The product was suspended in chloroform and separated by centrifugation at 5000 rpm. They were further washed with excessive chloroform for six times for the complete removal of unreacted *l*-lactic acid oligomer. After dried under a vacuum, *g*-HA particles were first suspended in chloroform and then well mixed with a 10% PLA/chloroform solution. The *g*-HA/PLA composite was obtained by a slow evaporation of chloroform followed by a vacuum-drying.

Thermogravimetric analyses of all materials were carried out using a Mettler Toledo TGA/SDTA851e (Mettler Toledo, Switzerland). Samples (20.0 mg) were heated from ambient temperature to 600 °C at various heating rates including 10, 15, 20 and 25 °C/min. A high purity nitrogen stream was continuously passed into the furnace at a flow rate of 50 ml/min.

All the data collected throughout the study were expressed as means ± standard deviations. Experimental data were analyzed using Microsoft Excel software. The difference was compared by a Student's *t*-test. A value of $P<0.05$ was considered statistically significant.

4. Results and discussion

Fig. 1 illustrates the TG and DTG curves for pure PLA and 10 wt% *g*-HA/PLA composite at 10 °C/min. The 5%, 10% and 50% weight loss temperatures (T_5, T_{10} and T_{50}, respectively) are listed in Table 2. The results indicate that the presence of *g*-HA had a mild enhancement in the thermal stability of PLA in the range of temperature

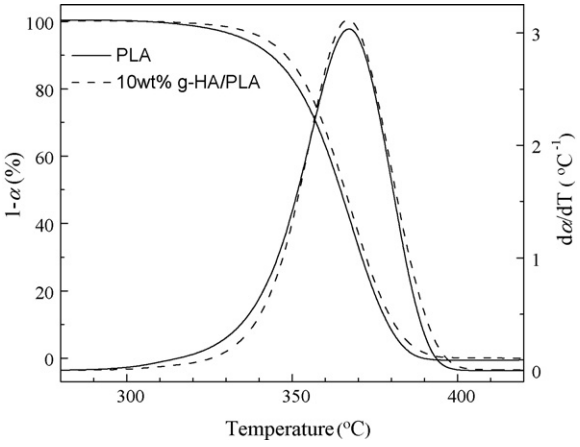

Fig. 1. TG and DTG curves of PLA and 10 wt% *g*-HA/PLA composite (heating rate: 10 °C/min).

Table 2
The T_5, T_{10} and T_{50} of PLA and 10 wt% *g*-HA/PLA composite at different heating rates.

	β (°C/min)	PLA	10 wt% *g*-HA/PLA
T_5	10	334.2	339.8
(°C)	15	342.4	344.3
	20	344.5	350.4
	25	356.0	355.0
Average		344.3	347.4
T_{10}	10	342.5	346.4
(°C)	15	350.3	351.4
	20	354.0	357.9
	25	363.0	362.4
Average		352.5	354.5
T_{50}	10	363.5	364.3
(°C)	15	370.3	370.4
	20	375.9	377.5
	25	382.5	382.1
Average		373.1	373.6

Table 3
T_p of PLA and the *g*-HA/PLA composite at different heating rates.

β (°C/min)	PLA (°C)	10 wt% *g*-HA/PLA (°C)
10	368.2	368.6
15	373.4	376.1
20	380.4	382.6
25	386.4	387.4

and heating rate investigated. It can be seen that the peak temperature of DTG, T_p, of both PLA and *g*-HA/PLA composite shifted to higher values with increasing heating rate (Table 3). However, there is no significant difference between T_p of PLA and the composite.

The *E* of the composite can be determined using the FWO method from a linear fitting of $\log \beta$ versus $1000/T$ at different conversion degrees α. Fig. 2 shows the activation energy of PLA and the *g*-HA/PLA composite at different conversion degrees. The activation energy of thermal degradation of two materials varies throughout the process. Thus, the thermal degradation of PLA and the composite could not proceed through a simple process. The activation energy of the composite is smaller than that of the polymer matrix, similar to the other studies [28–30]. The calculated *E* from FWO method were 166.0 ± 6.3 and 152.2 ± 7.0 kJ/mol for pure PLA and the *g*-HA/PLA composite, respectively. It can be attributed to the incorporation of *g*-HA into PLA caused a decrease in the degradation rate and an increase in the residual weight for the composite [29,30]. The activation energy of the PLA is 4.3–21.2% greater than that of the composite in the 0.3–0.9 weight loss region. It can be found that the *E* value of PLA increased from 155.3 to 169.7 kJ/mol at the first stage with an increase in α from 0.1 to 0.5, and then kept constant at about 170 kJ/mol until almost complete decomposition

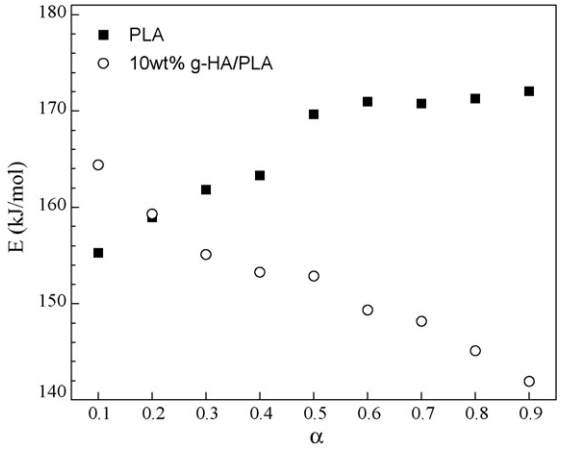

Fig. 2. *E* of PLA and the *g*-HA/PLA composite at different conversion degrees.

had occurred. Similar observations for PLA have also been reported [15,31] indicating that the degradation by both cis-elimination and ester interchange shifted towards cis-elimination with increase in temperature. The ester interchange has a lower energy of activation than the cis-elimination. Therefore, the values of *E* increased with α. Obviously, the derived kinetic parameters have to be considered as apparent values. When *g*-HA is present, the activation energy of the composite decreased with α (Fig. 2). This is mostly likely due to the existence of *g*-HA which is non-degradable in the range of temperatures investigated. Following the degradation of PLA, the content of *g*-HA that did not degrade increased. For a molar sample, the content of PLA, which consumed energy to be degraded during the thermal degradation, decreased. Because HA did not consume energy under 600 °C, the energy for the thermal degradation of a molar sample, i.e. *E*, decreased.

The IKP method allows us to compute the invariant activation energy, invariant pre-exponential factor and model the thermal degradation of the material. In this work, eighteen apparent activation energies ($E_{j\nu}$) and pre-exponential factors ($A_{j\nu}$) were calculated using the Coats-Redfern method. For each heating rate, the activation parameters were correlated through the compensation effect relationship given in Eq. (7). The values of the compensation parameters (B_ν and I_ν) and the invariant kinetic parameters (A_{inv} and E_{inv}) for PLA and the composite are listed in Table 4. It can be seen that the activation energy values obtained by the IKP method were in good agreement with the values obtained by FWO method. Values of PLA and the composite are significantly different ($P < 0.05$) according to the Student's *t*-test.

The degradation of a polymeric material often cannot be represented by a single function, but by a set of functions because of the different processes which can occur during the degradation of the material.

Table 4
The values of compensation effect parameters and invariant kinetic parameters for PLA and the 10 wt% *g*-HA/PLA composite.

β (°C/min)	B_ν (A, S^{-1})	I_ν (mol/kJ)	R	E_{inv} (kJ/mol)	$\log A_{inv}$ (A, S^{-1})
PLA					
10	-2.34 ± 0.13	0.082 ± 0.00048	0.9997		
15	-2.15 ± 0.13	0.081 ± 0.00046	0.9997	174.7 ± 16.5	11.92 ± 1.33
20	-2.04 ± 0.12	0.080 ± 0.00041	0.9998		
25	-1.93 ± 0.13	0.079 ± 0.00044	0.9998		
g-HA/PLA					
10	-2.29 ± 0.13	0.081 ± 0.00043	0.9998		
15	-2.15 ± 0.13	0.081 ± 0.00045	0.9998	139.3 ± 13.0	9.06 ± 1.04
20	-2.06 ± 0.13	0.080 ± 0.00048	0.9997		
25	-1.96 ± 0.13	0.079 ± 0.00047	0.9997		

Table 5
The probability distributions of the kinetic degradation functions of PLA and the *g*-HA/PLA composite.

PLA		10 wt% *g*-HA/PLA	
Type	Probability (%)	Type	Probability (%)
S1	0	S1	0
S2	33.4	S2	44.0
S3	0.5	S3	0.7
S4	0	S4	0
S5	0	S5	0
S6	2.7	S6	3.9
S7	0	S7	0
S8	0	S8	0
S9	6.7	S9	0.9
S10	0	S10	0
S11	0	S11	0
S12	0	S12	0
S13	0	S13	0
S14	0	S14	0
S15	30.6	S15	8.6
S16	0	S16	0
S17	26.0	S17	41.8
S18	0	S18	0

The IKP method allows us to compute the probability distribution associated with the kinetic function and therefore, gives a probable guide to the degradation of the material. The probabilities associated with each kinetic function were calculated (Table 5). The probability distributions for PLA and the composite showed that the thermal degradation might be represented by a set of probable kinetic functions. And the degradation functions $f(\alpha)$ of PLA and the composite might be modeled by Eqs. (15) and (16), respectively:

$$f_{\mathrm{PLA}}(\alpha) = 0.334 \times 3(1-\alpha)(-\ln(1-\alpha))^{2/3} + 0.005 \times 2(1-\alpha)(-\ln(1-\alpha))^{1/2} + 0.067 \times \frac{1}{2}\alpha^{-1} + 0.306 \times 2(1-\alpha)^{1/2} + 0.260 \times \frac{2}{3}\alpha^{-1/2} + 0.027 \quad (15)$$

$$f_{g-\mathrm{HA/PLA}}(\alpha) = 0.440 \times 3(1-\alpha)(-\ln(1-\alpha))^{2/3} + 0.007 \times 2(1-\alpha)(-\ln(1-\alpha))^{1/2} + 0.009 \times \frac{1}{2}\alpha^{-1} + 0.086 \times 2(1-\alpha)^{1/2} + 0.418 \times \frac{2}{3}\alpha^{-1/2} + 0.039 \quad (16)$$

It shows that the mechanisms of degradation were complex and that it did not degrade following an elementary law. The thermal degradations of PLA [15] and the composite could not be represented by a single function, but by a set of functions. The thermal degradation of PLA and the composite could mainly be modeled by a nucleation and nucleus growing (S2), reaction order (S15) and potential law (S17) mechanism. Basic process determining rates for PLA (Table 5) are nucleation and nucleus growing (S2), reaction order (S15) and potential law (S17) mechanism. For the composite, the effect of nucleation and nucleus growing (S2) and potential law (S17) mechanism on the degradation rate obviously intensified. However, diffusion (S9) and reaction order (S15) mechanism effect weakened. The reason is that *g*-HA filler particles have barrier effect to slow down product volatilization and thermal transport [32].

The degradation rates versus α and T are plotted in Fig. 3, where

$$\text{the degradation rate} = A_{inv} \exp\left(-\frac{E_{inv}}{RT}\right) \sum_{j=1}^{18} f_j(\alpha_j)$$

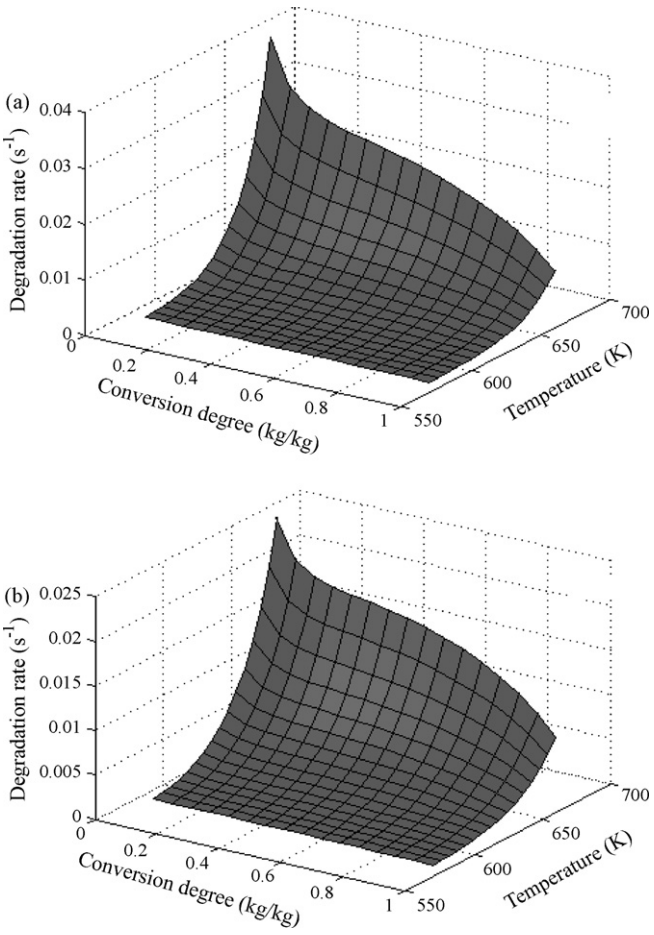

Fig. 3. Thermal degradation rate of PLA (a) and the *g*-HA composite (b) versus conversion degree and temperature plots.

An increase in the rate of the thermal degradation of PLA and the composite versus temperature plot is shown in Fig. 3. At high temperature the rate of thermal degradation decreased when the conversion degree values increased. This kind of behavior had already been observed [33]. The results exhibit that the system degraded rapidly to form material which would act as a protective shield. The degradation mechanism is a mixture of reaction order and potential law, which is in agreement with the degradation of a polymeric material leading to the development of a protective shield.

The degradation rate of the composite was lower than that of pure PLA (Fig. 3), similar to other studies [32,34,35]. The mechanism of thermal degradation of PLA is more complex than the simple polymerization/depolymerization equilibrium. Generally, inter- and intra-molecular transesterification reactions are considered as the principal mechanism of PLA pyrolysis [14,15,36]. Other reactions, such as cis-elimination and non-selective radical reaction, can also occur competitively. For the composite, *g*-HA has an adverse effect on intra-molecular transesterification as a barrier. The backbiting ester interchange reaction will be slowed down due to the existence of *g*-HA. During decomposition of the polymer matrix, *g*-HA filler particles also have barrier effect to slow down product volatilization and thermal transport, which assists composites with high thermal stability [32]. Furthermore, the adsorption of polymer chains onto the surface of *g*-HA particles hinders the internal rotation of high molecular chain segments, results in restriction of segmental mobility and serves to suppress redistribution and chain transfer reactions [32,35].

5. Conclusions

In this paper, the thermal degradations of PLA and the *g*-HA/PLA composite were studied in a nitrogen atmosphere. The results indicated that the incorporation of *g*-HA particles can increase the thermal stability of PLA.

Kinetic study using both IKP and FWO methods revealed a lower activation energy of *g*-HA/PLA composite than that of PLA, and the activation energy values obtained by both methods were in good agreement. The thermal degradations of PLA and the composite could be represented by some functions using the IKP method. However establishing a certain reaction model is impossible based on the results obtained in this study. Complementary proof from other experiments is needed for the comprehensive understanding of the thermal degradation process of the composite materials.

Acknowledgement

This work is supported by the Research Fund for the Doctoral Program of Higher Education of China (20060217012).

References

[1] S.H. Teng, E.J. Lee, P. Wang, H.E. Kim, Mater. Lett. 62 (2008) 3055.
[2] X.G. Miao, D.M. Tan, J. Li, Y. Xiao, R. Crawford, Acta Biomater. 4 (2008) 638.
[3] J.Q. Wen, Y.B. Li, Y. Zuo, G. Zhou, J.F. Li, L.Y. Jiang, W. Xu, Mater. Lett. 62 (2008) 3307.
[4] D.Z. Chen, C.Y. Tang, K.C. Chan, C.P. Tsui, P.H.F. Yu, M.C.P. Leung, P.S. Uskokovic, Compos. Sci. Technol. 67 (2007) 1617.
[5] S.S. Liao, W. Wang, M. Uo, S. Ohkawa, T. Akasaka, K. Tamura, F.Z. Cui, F. Watari, Biomaterials 26 (2005) 7564.
[6] C.Y. Tang, D.Z. Chen, T.M. Yue, K.C. Chan, C.P. Tsui, P.H.F. Yu, Compos. Sci. Technol. 68 (2008) 1927.
[7] P.S. Uskokovic, C.Y. Tang, C.P. Tsui, N. Ignjatovic, D.P. Uskokovic, J. Eur. Ceram. Soc. 27 (2007) 1559.
[8] Y. Shikinami, M. Okuno, Biomaterials 22 (2001) 3197.
[9] P.L. Lin, H.W. Fang, T. Tseng, W.H. Lee, Mater. Lett. 61 (2007) 3009.
[10] J.I. Velasco, J.A.D. Saja, A.B. Martínez, J. Appl. Polym. Sci. 61 (1996) 125.
[11] W.L. Qiu, K.C. Mai, H.M. Zeng, J. Appl. Polym. Sci. 71 (1999) 1537.
[12] Q. Liu, J.R.D. Wijn, C.A.V. Blitterswijk, J. Biomed. Mater. Res. 40 (1998) 490.
[13] J. Li, X.L. Lu, Y.F. Zheng, Appl. Surf. Sci. 255 (2008) 494.
[14] I.C. McNeill, H.A. Leiper, Polym. Degrad. Stabil. 11 (1985) 309.
[15] F.D. Kopinke, M. Remmler, K. Mackenzie, M. Möder, O. Wachsen, Polym. Degrad. Stabil. 53 (1996) 329.
[16] Y. Aoyagi, K. Yamashita, Y. Doi, Polym. Degrad. Stabil. 76 (2002) 53.
[17] A. Babanalbandi, D.J.T. Hill, D.S. Hunter, L. Kettle, Polym. Int. 48 (1999) 980.
[18] D.F. Wu, L. Wu, M. Zhang, Y.L. Zhao, Polym. Degrad. Stabil. 93 (2008) 1577.
[19] D.F. Wu, L. Wu, L.F. Wu, M. Zhang, Polym. Degrad. Stabil. 91 (2006) 3149.
[20] J.H. Flynn, L.A. Wall, J. Polym. Sci. Part B: Polym. Lett. 4 (1966) 323.
[21] T. Ozawa, Bull. Chem. Soc. Jpn. 38 (1965) 1881.
[22] A.I. Lesnikovich, S.V. Levchik, J. Therm. Anal. Calorim. 27 (1983) 89.
[23] A.I. Lesnikovich, S.V. Levchik, J. Therm. Anal. Calorim. 30 (1985) 677.
[24] A.W. Coats, J.P. Redfern, Nature 201 (1964) 68.
[25] A.I. Lesnikovich, S.V. Levchik, V.G. Guslev, Thermochim. Acta 77 (1984) 357.
[26] L. Richard-Campisi, S. Bourbigot, M.L. Bras, R. Delobel, Thermochim. Acta 275 (1996) 37.
[27] R.K. Kulkarni, E.G. Moore, A.F. Hegyeli, J. Biomed. Mater. Res. 5 (1971) 169.
[28] T.C.K. Yang, S.S.Y. Lin, T.H. Chuang, Polym. Degrad. Stabil. 78 (2002) 525.
[29] E.C. Chen, T.M. Wu, Polym. Degrad. Stabil. 92 (2007) 1009.
[30] S.C. Liufu, H.N. Xiao, Y.P. Li, Polym. Degrad. Stabil. 87 (2005) 103.
[31] Y.J. Fan, H. Nishida, S. Hoshihara, Y. Shirai, Y. Tokiwa, T. Endo, Polym. Degrad. Stabil. 79 (2003) 547.
[32] J. Kuljanin-Jakovljević, M. Marinović-Cincović, Z. Stojanović, A. Krklješ, N.D. Abazović, M.I. Čomor, Polym. Degrad. Stabil 94 (2009) 891.
[33] X. Almeras, F. Dabrowski, M.L. Bras, R. Delobel, S. Bourbigot, G. Marosi, P. Anna, Polym. Degrad. Stabil. 77 (2002) 315.
[34] Q.Y. Zhou, M. Xanthos, Polym. Degrad. Stabil. 94 (2009) 327.
[35] Yilser Devrim, Serdar Erkan, Nurcan Baç, Inci Eroğlu, Int. J. Hydrogen Energy 34 (2009) 3467.
[36] O. Wachsen, K. Platkowski, K.H. Reichert, Polym. Degrad. Stabil. 57 (1997) 87.